GEOPHYSICAL RESEARCH LETTERS, VOL. 29, NO. 4, 1054, 10.1029/2001GL013987, 2002

Simulation of sedimentary rock deformation: Lab-scale model calibration and parameterization

David F. Boutt and Brian J. O. L. McPherson

New Mexico Institute of Mining and Technology, Department of Earth and Environmental Science, Hydrology Program and Petroleum Recovery Research Center, Socorro, NM, Mexico

Received 24 August 2001; revised 13 November 2001; accepted 13 November 2001; published 28 February 2002.

[1] Understanding the mechanical behavior of rock is critical for researchers and decision-makers in fields from petroleum recovery to hazardous waste disposal. Traditional continuum-based numerical models are hampered by inadequate constitutive relationships governing fracture initiation and growth. To overcome limits associated with continuum models we employed a discrete model based on the fundamental laws of contact physics to calibrate triaxial tests. Results from simulations of triaxial compression tests on a suite of sedimentary rocks indicate that the basic physics of rock behavior are clearly captured. Evidence for this conclusion lie in the fact that one set of model parameters describes rock behavior at many confining pressures. The use of both inelastic and elastic parameters for comparison yields insight concerning the uniqueness of these models. These tests will facilitate development and calibration of larger scale discrete element models, which may be applied to a wide range of geological problems. *INDEX TERMS:* 5112 Physical Properties of Rocks: Microstructure; 5104 Physical Properties of Rocks: Fracture and flow; 8020 Structural Geology: Mechanics; 8094 Structural Geology: Instruments and techniques

1. Introduction

[2] The mechanical behavior of sedimentary rocks is an important aspect of many investigations in the earth sciences. Previous workers analyzed these behaviors in the laboratory and made fundamental advancements (See *Lockner* [1995] for review). This paper highlights an investigation of the micromechanical behavior of sedimentary rocks using the discrete element method (DEM) [*Cundall*, 1971; *Cundall and Strack*, 1979]. This type of DEM simulates the mechanical behavior of rock by idealizing the system as a collection of structural units (springs, beams, etc.) or separate particles bonded together at their contact points, and utilizes the breakage of individual structural units or bonds to represent damage. The DEM successfully modeled the behavior of rocks, particularly damage and non-linear behaviors, by employing simple contact models [*Potyondy et al.*, 1996; *Hazzard et al.*, 2000]. Models that explicitly include damage are unique and far more robust than models that indirectly represent damage through empirical relations, such as continuum models. In the DEM constitutive behaviors are results rather than assumptions.

[3] This study builds on previous DEM studies by exploring model behavior at a variety of stress states through attempting to explicitly reproduce select rock behavioral properties and to identify correlations between model results and observed rock behavior. In examining a variety of stress states we found that particle clustering (groups of bonded particles) allow a more expanded range of micromechanical behaviors. In addition by examining multiple stress states we determined important microparameter relationships not otherwise detected.

0094-8276/02/2001GL013987S05.00

2. Modeling Approach

2.1. Limitations of Previous DEM Studies

[4] Previous DEM studies [*Hazzard et al.*, 2000; *Bruno and Nelson*, 1991; *Wang et al.*, 2000; *Potyondy et al.*, 1996] of laboratory scale mechanical behavior examined very limited sets of tests under similar stress fields. Results of these tests and simulations may be too specific to the chosen tested stress states and not adequately represent general rock behavior. In many cases the microparameters (i.e., DEM model parameters) that govern macroscopic rock behavior reproduce the specific stress state, but do not provide a complete failure envelope. A more robust approach is to use many stress states to define the relevant microparameters (i.e., macroscopic rock properties). This would result in a more complete comparison and also reduce the number of degrees of freedom. Other researchers, including *Li and Holt* [2001] examined compaction and dilation of highly porous rock at different confining pressures, but did not compare model results to laboratory test data.

2.2. Selection of Parameters to Calibrate

[5] For our purposes, the most important material properties to calibrate are the elastic and inelastic rock properties, including Youngs modulus, Poissons ratio, failure strength (at many confining pressures), and style of failure (uniaxial splitting or shear faulting, cataclastic flow, ductile). The style of failure is very important in a rock deformation model since it is an explicit control on the distribution of brittle deformation taking place. We have observed that strain localization in our models of rock can be somewhat distributed and ductile in nature and still match the observed elastic and inelastic parameters. Thus it is important to replicate both elastic and inelastic strain accumulation. An exact match to the shape of the stress-strain curve is not appropriate since most rocks undergo some inelastic deformation during laboratory tests due to flaws in addition to the inherent randomness of both samples and models.

2.3. Methods

[6] We are using a commercially available DEM code called Particle Flow Code 2D (PFC2D), developed by Itasca Consulting Group, Inc. A detailed description of the 2-dimensional PFC model and the theory is provided by *Hazzard et al.* [2000]. Mechanical measurements of a suite of sedimentary rocks from the Midland Basin, Texas were selected for analysis. The Midland Basin rocks vary in lithology from fine-grained sandstones to laminated mudstones with little matrix porosity and exhibit a wide range of unconfined failure strengths (between 137 MPa to 220 MPa). For more details concerning the rocks, associated properties and data collection see *Lorenz et al.* [2001] and *Sterling* [2000].

[7] Laboratory conditions are explicitly reproduced in the model including servo controlled confining pressure, platen velocity, and sample size. The particle size distribution was normally distributed with the smallest particle being 1 mm and the largest

Table 1. Input Microparameters for DEM Models

Core Location	Bond Modulus (GPa)	P-bond Normal Strength (MPa)	P-bond to C-bond Strength Ratio	Cluster Size
1U-1	23.5	18	0.75	3
5U-3	13.5	10.45	0.5	2
5U-4	23.5	10.5	0.75	3
5U-6	22	12.5	0.5	2

being 1.66 mm in an area of 2.54 cm wide by 5.08 cm long. We do not stipulate a single particle to represent a single rock grain, but rather the assembly represents a collection of spatially averaged grains [*Hazzard et al.*, 2000]. Each model therefore consisted of roughly 1000 particles giving an average of 22 particles along the shortest dimension of the model. This number of particles ensures the model is not sensitive to our choice in particle size, using criteria of *Huang et al.* [1999].

[8] Table 1 shows the values of input microparameters for each of the 4 models. The moduli of all particles and bonds within the respective model were set to the value given in the table. All bonds within clusters had 650 MPa strength magnitudes, where bonds between clusters had shear to normal bond strength ratios of 8 and magnitudes as summarized in the table. Cluster size varied between 2 and 3 for the models shown. Preliminary work on effects of cluster geometry indicates that it has a strong influence on the slope of the compressional strength envelope.

3. Results and Discussion

3.1. General Relationships Among Microparameters and Macroparameters

[9] Our procedure for attempting to reproduce the rock behavior began with an extensive sensitivity study attempting to elucidate which microparameters exerted the strongest control on the macroparameters of interest. Figure 1 describes what microparameters were found to control which macroscopic model behaviors (macroparameters). The particle friction coefficient and particle clustering attributes were found to increase the slope of the compressive failure envelope. "Particle clustering" [*Potyondy*, 1999] refers to the process of bonding 2 or more particles with a normal and shear strength greater than the strengths of the bonds between the clusters themselves (inter-cluster bonds). In practical terms, clustering is intended to make the DEM particles or particle clusters more closely mimic the mechanical behavior of rock grains or groups of grains. This results in an increase in failure strength of the higher confining pressure samples possibly due to interlocking of the clusters [Boutt and McPherson, 2001]. We suggest that the particle friction coefficient has a similar effect on failure strength. For all models in this study the particle friction coefficient was held constant at a value of 0.5.

[10] The normal and shear contact and bond stiffness control the elastic parameters, with the ratio of the shear to normal stiffnesses having a larger effect on the exhibited Poissons ratio of the assembly. The parallel and contact bond strength of the inter-cluster bonds of a clustered material is set such that it controls the uniaxial compressional strength with the particle clustering controling the slope of the failure envelope. Parallel bonds (rectangular feature in Figure 1) are bonds that act over a specified area of the two particles in contact and can transmit a moment in addition to a force onto the particles.

3.2. Calibration of Failure Mode

[11] Our initial modeling efforts suggested that even though quantitative and consistent calibrations between the simulated and observed material properties were possible, the type and mode of failure was quite different in the model than those measured or observed in the actual rock deformation tests. In some cases a somewhat non-localized ductile type of failure was observed. We believe that the model assembly was failing in a non-localized manner because shear and normal bond strengths were similar. The model was failing preferentially through shear bond breakages, whereas failure and localization depend on differential stress and interparticle shear strength. Models with high ratios of shear to normal bond strength (>4) produce a well defined shear plane, as illustrated in Figure 2. A similar conclusion was documented by *Huang et al.* [1999]. In summary, the ratio of shear to normal bond strength in the DEM plays an important role in strain localization. By using quantitative (and qualitative) measures of inelastic processes in addition to elastic properties for comparison we derive microparameter relationships that are otherwise undeterminable.

[12] The evolution of strain localization in a modeled sample via a through-cutting shear fault is depicted for a sample under uniaxial stress in Figure 2. In this plot gradients of displacement are contoured to emphasize areas undergoing differential movement [*Morgan and Boettcher*, 1999]. A stark contrast in displacement gradient magnitudes indicates that regions on either side are moving coherently. The gradients are then plotted at different times throughout the test and are related to the axial stress-strain plot by the numbers above the individual plot. Before peak stress, stage 1 through 2, the sample exhibits very low magnitudes of displacement gradients. A slight amount of localization is developed in stage 3 where a linear feature first appears. At peak stress, stage 4, the sample begins to show displacement gradients that resemble a failure plane. Stages 5 through 7 show the post peak behavior where the through going shear fault is realized and destruction of the sample begins by development of splays off the main fault. This is consistent with our laboratory observations and with the results of *Menendez et al.* [1996]. Progression of strain localization in the modeled samples is captured with the calculated displacement gradients which indicate a good match between the model and laboratory observations.

3.3. Strength Envelopes

[13] Using the above results as a guide, we used an iterative process in an attempt to mimic the full compressive strength

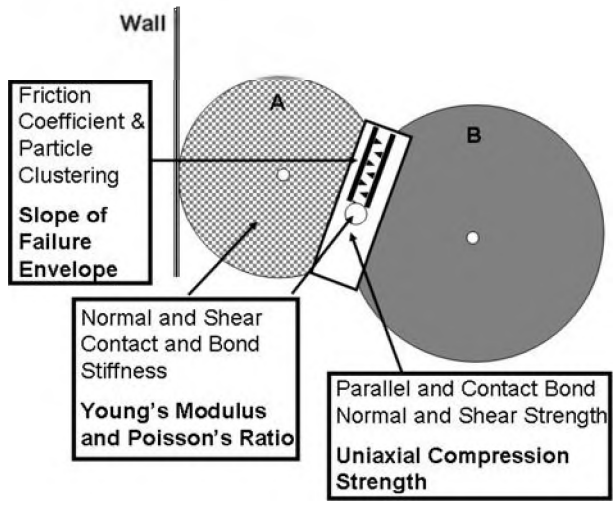

Figure 1. Example of particle to particle interaction and model assembly. Particles interact with a series of contact and bonding models specified by normal and shear properties, such as stiffness and bond strength.

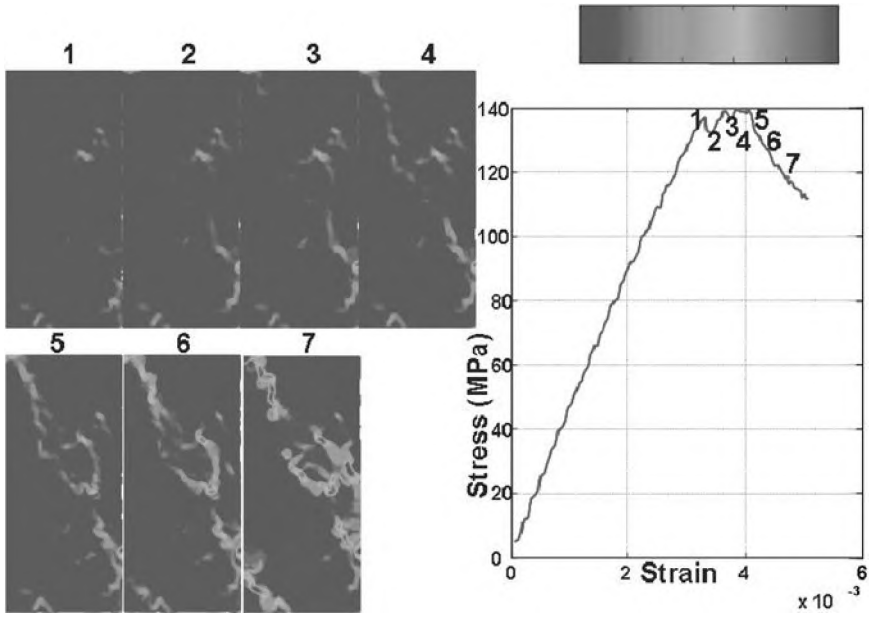

Figure 2. Time series of displacement gradients (see text) for sample 5U-4 at 0 MPa confining pressure. The localization in the modeled sample evolves from a distributed mode (dark colors) of very little deformation to a highly localized deformation (light colors) just after peak stress. This zone is approximately 4 particles wide.

envelope of the rock as well as appropriate failure modes, using a single and unique set of micro-parameters. This entailed generating multiple DEM assemblies with the same microparameters and running simulations at the same confining pressures as the laboratory tests. Figure 3 shows the comparison between simulated and observed compressive failure envelopes for 3 different rock samples, at various confining pressures. The match is qualitatively consistent – the differences in the model results compared to the laboratory tests are well within the reproducibility of the laboratory test results. The changes in slopes between adjacent points of the same modeled samples are very different, especially at small confining pressures. This difference in slope may be attributed to how the model accomodates different levels of stresses. This is not observed in un-clustered material and may represent a systematic stress response of the different size clusters. The clustered material appears to increase the overall slope of the compressive failure envelope, which is not attainable using unclustered material and realistic microparameters.

3.4. Stress-Strain Curves

[14] In the DEM model, we calibrated the slope of the stress-strain curves to the intrinsic elastic properties of the rock. Both the observed and simulated differential stress vs. axial strain and volumetric strain vs. axial strain including load-unload loops are plotted in Figure 4 (See *Jaeger and Cook*, 1969 for discussion of load-unload loops). The dashed lines indicate the curves for the simulated rock and the solid line the observed rock. Since the model is calibrated to the intrinsic elastic properties and not the damaged rock the stress-strain curves take on different forms, as illustrated in Figure 4a. Much more strain is observed in the real rock due to processes not captured in the simulated rock, such as grain boundary sliding and preexisting cracks.

[15] The plots of volumetric strain vs. axial strain (Figure 4b) highlight volume changes in the samples over the course of the triaxial tests. As sample loading begins initial compaction takes place (positive volumetric strain) until approximately 90% axial strain, then a sharp increase in volume occurs. This is documented in both the laboratory and the model and is termed shear enhanced dilation, common in low porosity fined grained sedimentary rocks [*Brace*, 1978; *Wong et al.*, 1992]. The simulated and observed stress-strain curves are quite similar in terms of their general trends in volume changes as well as timing of these events.

[16] The post peak behaviors in the simulated samples are quite different than in the laboratory as shown in Figure 4. This may be best explained by considering the stiffness of the testing machine vs. the model stiffness. In a very compliant system, as typically most triaxial compression devices are [*Shimamoto et al.*, 1980], a significant amount of energy is absorbed in the machine and consequently released upon failure of the sample. This energy causes inertial effects in the sample, rapid propagation of the shear fracture, and a steep drop in stress. Post peak comparison of stress-

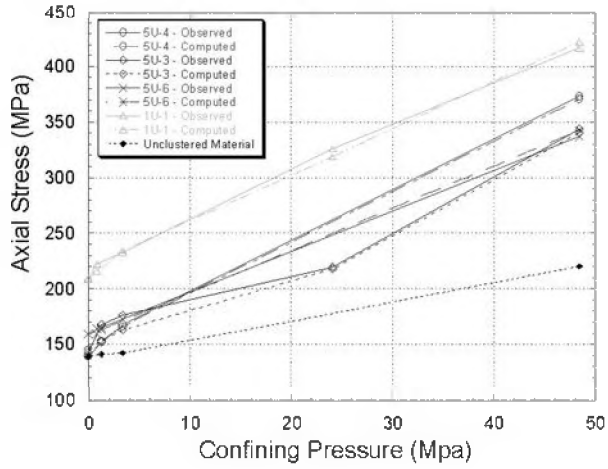

Figure 3. Simulated and observed compressive failure envelopes for 4 different groups of sedimentary rocks from the Midland Basin. Failure envelopes were determined by plotting peak stress at the given confining pressure. A good match is achieved through adjusting the main parameters controlling the slope of the compressive failure envelope, particle friction (0.5 in all models) and cluster size. Note the difference in slope between the unclustered material and the models in this study.

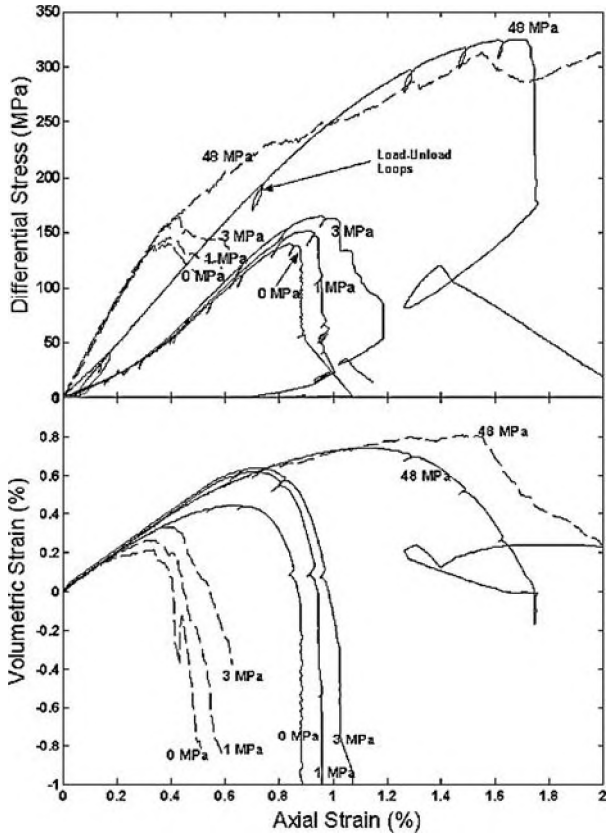

Figure 4. Simulated and observed axial stress and volumetric strain vs. axial strain curves for sample 5U-4. Solid lines represent observed laboratory data at the confining pressure marked on the plot and dashed lines represent the simulated data. Differences in the position of the curves along the x axis are due to a choice in elastic parameter calibration (intrinsic vs. damaged rock properties). The general trends in the curves are clearly captured.

strain curves using data from a non-stiff triaixal machine is not possible with a model not considering those same processes.

4. Conclusions

[17] The numerical approximation of the mechanical behavior of rock is difficult using traditional continuum based models that often are hampered by inadequate constitutive relationships governing crack initiation and growth. The discrete model applied in this study has been shown to match the observed laboratory data very well with model microparameters chosen by comparing elastic and inelastic material behavior. Calibrated models of rock behavior could be used to explore scaling relationships as well as provide insight into the micromechanics of rock fracture.

[18] The modeled progression of strain localization in the samples is clearly captured with the calculated displacement gradients that indicate a good match between the model and laboratory observations. Post peak comparison of stress-strain curves using data from a non-stiff triaxial machine is not possible. The ratio of shear to normal bond strength in the DEM plays an important role in strain localization. Clustered material appears to increase the overall slope of the compressive failure envelope, which is unattainable using un-clustered material and realistic microparameters. The simulated and observed stress-strain curves are quite similar in terms of their general trends in volume changes as well as timing of these events. Finally, by utilizing more than one calibration parameter, looking at failure envelopes and failure modes, we have identified microparameter relationships that would not be apparent otherwise.

[19] **Acknowledgments.** This work was supported by funds from the New Mexico Tech Petroleum Recovery Research Center.

References

Brace, W. F., Volume changes during fracture and frictional sliding: A review, *Pure Appl. Geophys.*, *116*, 603–614, 1978.

Bruno, M. S., and R. B. Nelson, Microstructural Analysis of the Inelastic Behavior of Sedimentary Rock, *Mechanics of Materials*, *12*, 95–118, 1991.

Cundall, P. A., A computer model for simulating progressive, large-scale movement in block rock systems, Proc Symp. Int. Soc. Rock Mech., Nancy 2, 1971.

Cundall, P. A., and O. D. L. Strack, A discrete element model for granular assemblies, *Geotechnique*, *29*(1), 47–65, 1979.

Hazzard, J. F., R. P. Young, and S. C. Maxwell, Micromechanical modeling of cracking and failure in brittle rocks, *J. Geophys. Res.*, *105*, 16,683–16,697, 2000.

Huang, H., E. Detournay, and B. Bellier, Discrete Element Modeling of Rock Cutting, in Rock Mechanics for Industry, edited by Amadei, Kranz, Scott, and Smealie, pp. 123–130, Balkema, Rotterdam, 1999.

Jaeger, J. C., and N. G .W. Cook, Fundamentals of Rock Mechanics, 585 pp., Chapman and Hall, London, 1969.

Li, L., and R. M. Holt, Simulation of granular material using particle model with non-circularly shaped super-particles, in Proc. EUROCK'2001: Rock Mechanics - a Challenge for Society, edited by P. Srkk, and P. Eloranta, pp. 511–516, A. A Balkema, Rotterdam, 2001.

Lockner, D. A., Rock Failure, in Rock physcis and phase relations: A handbook of physcial constants, edited by T. J. Ahrens, pp. 295, AGU, Washington, 1995.

Lorenz, J. C., J. L. Sterling, D. S. Schecter, C. L. Whigham, and J. L. Jensen, Natural Fractures in the Spraberry Formation, Midland Basin, Tx: The Effects of Mechanical Stratigraphy on Fracture Variability and Reservoir Behavior, AAPG Bulletin, in review.

Menendez, B., W. Zhu, and T.-f. Wong, Micromechanics of brittle faulting and cataclastic flow in Berea sandstone, *J. Structural Geology*, *18*(1), 1–16, 1996.

Morgan, J., and M. S. Boettcher, Numerical simulations of granular shear zones using the distinct element method 1. Shear zone kinematics and the micromechanics of localization, *J. Geophys. Res.*, *104*, 2703–2719, 1999.

Potyondy, D. O., Fish in PFC2D, Itasca Consulting Group, Minneapolis, 1999.

Potyondy, D. O., P. A. Cundall, and C. A. Lee, Modeling rock using bonded assemblies of circular particles, in Rock Mechanics: Tools and Techniques, edited by Aubertin, Hassani, and Mitri, pp. 1937–1944, Balkema, Rotterdam, 1996.

Shimamoto, T., J. Handin, and J. M. Logan, Specimen-Apparatus Interaction During Stick-Slip in a Triaxial Compression Machine: A Decoupled Two-Degree-Of-Freedom Model, *Tectonophysics*, *67*, 175–205, 1980.

Sterling, J. L., Fracture generation and fluids in the Spraberry Formation, Midland Basin, Texas, Independent Study Thesis, New Mexico Institute of Mining and Technology, Socorro, NM, 2000.

Wang, Y.-C., X.-C. Yin, F.-J. Ke, M.-F. Xia, and K.-Y. Peng, Numerical simulation of rock failure and earthquake process on mesoscopic scale, *Pure and Apllied Geophysics*, *157*, 1905–1928, 2000.

Wong, T.-f., H. Szeto, and J. Zhang, Effect of loading path and porosity on the failure mode of porous rocks, *Appl. Mech. Rev.*, *45*, 281–293, 1992.

David F. Boutt and Brian J. O. L. McPherson, New Mexico Institute of Mining and Technology, Hydrology Program, Petroleum Recovery Research Center Department of Earth and Environmental Science, Socorro, New Mexico 87801. (dboutt@nmt.edu)